

# UltraButton: A Minimalist Touchless Multimodal Haptic Button

Rafael Morales<sup>1</sup>, Dario Pittera<sup>1</sup>, Orestis Georgiou<sup>1</sup>, Brian Kappus<sup>1</sup>, and William Frier<sup>1</sup>  
<sup>1</sup>Ultraleap Ltd., Bristol BS2 0EL, UK

We present *UltraButton* a minimalist touchless button including haptic, audio and visual feedback costing only \$200. While current mid-air haptic devices can be too bulky and expensive (around \$2k) to be integrated into simple mid-air interfaces such as point and select, we show how a clever arrangement of 83 ultrasound transducers and a new modulation algorithm can produce compelling mid-air haptic feedback and parametric audio at a minimal cost. To validate our prototype, we compared its haptic output to a commercially-available mid-air haptic device through force balance measurements and user perceived strength ratings and found no significant differences. With the addition of 20 RGB LEDs, a proximity sensor and other off-the-shelf electronics, we then propose a complete solution for a simple multimodal touchless button interface. We tested this interface in a second experiment that investigated user gestures and their dependence on system parameters such as the haptic and visual activation times and heights above the device. Finally, we discuss new interactions and applications scenarios for *UltraButtons*.

## I. INTRODUCTION

Touchless interfaces such as mid-air buttons enable users to interact with systems without needing to physically touch a surface. Driven at first by science fiction movies such as *Minority Report* or *Iron Man*, the interest in touchless interfaces has increased in recent years when experimental studies showed that touchscreens in public spaces form a pathogen vector for bacterial and viral propagation [1]–[3]. This aspect has been exacerbated by the recent Covid-19 pandemic [4], [5].

Despite all this, touchless interfaces are still at their infancy, and their associated interaction paradigms remains limited. For instance, in a simple point and select task, touchless interfaces using a gesture tracking system as their main input modality need to differentiate between “pointing” and “selecting” actions. Thus the usability of touchless systems suffers from both a lack of gesture input standardisation and a lack of haptic feedback – the act of action confirmation to the user [6]. Touchless digital kiosks and large public displays circumvent this issue by relying on advanced visual and audio feedforward and feedback (e.g., visual animation) [7]. Simpler touchless systems may not include such large screens and high definition visuals and instead rely on very basic visual and auditory cues such as LED blinks and audio beeps.

In this paper, our aim is to enhance simple touchless interfaces with ultrasound mid-air haptic feedback [8] and parametric audio [9] capabilities. Mid-air haptic displays have been the focus of numerous studies (there are over 100 papers to date) – see a recent survey here [10]. Moreover, mid-air haptic displays are commercially available and can accurately deliver dynamic tactile feedback to users’ palms and fingertips at a range of up to 1 meter. This is usually achieved

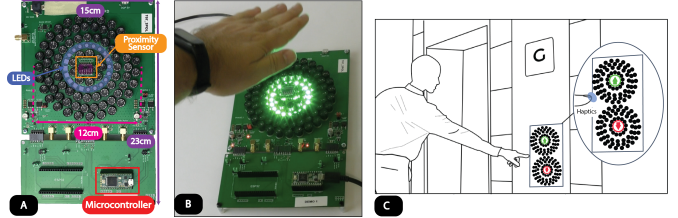


Fig. 1: *UltraButton* prototype and proof-of-concept applications. A) Arrangement of 83 transducers, multi-colour LEDs, a central proximity sensor, and a microcontroller. Dimensions of the device are 230mm length by 150mm width and the diameter of the transducer’s arrangement is 120mm. B) Application of simple button click interaction with visual feedforward technique and haptic feedback. C) Concept of touchless multimodal haptic interface.

by focusing algorithms applied to phased arrays comprising hundreds of ultrasound transducers. Studies have shown that by providing mid-air haptic feedback to infotainment systems in cars [11], digital kiosks and pervasive displays [12], user performance and experience can be improved significantly. Notably, ultrasound phased arrays have recently been able to generate multimodal volumetric displays for visual, tactile and audio presentation using acoustic trapping techniques [13], [14]. While such devices can enhance touchless systems with rich haptic feedback, building them can be expensive due to the large number of transducers needed and the embedded micro-electronics used for manipulating individual phases and amplitudes. This high cost of the current generation of mid-air haptic displays may thus render them unsuitable for small and simple touchless interactive applications.

Despite there being much progress in the field of mid-air displays, the efforts to date have mostly been geared towards bigger and better [15]. Sometimes, however, less is more. Our goal here is to design and build a minimal-cost (in terms of dollars, power, and compute) mid-air haptic button with similar haptic strength as commercial alternatives yet remains practical and functional for simple touchless interaction scenarios. Our approach is guided by a simplification of the driving circuitry, a fixed-in-space mid-air haptic focal point, and a reduction in the number of transducers used, while still maintaining the ability to deliver a multi-modal output (visual, auditory and haptic feedback). To that end, we introduce a new and simple design for the generation of haptic buttons in mid-air — the *UltraButton* — the features and design of which we think can influence future touchless interfaces and market directions.

This paper describes the system and methods for creating an interactive mid-air button and its evaluations. The main contributions of this paper are: 1) A low-cost hardware design for creating a mid-air haptic *UltraButton* (see Figure 1a). 2) A novel haptic algorithm for creating perceivable mid-air haptic sensations. 3) Multiple quantitative and qualitative evaluations of our multimodal mid-air haptic system. 4) An exploration of the use cases enabled by the *UltraButton*.

## II. RELATED WORK

### A. Ultrasonic haptic devices

Ultrasonic mid-air haptic devices are based on a nonlinear phenomenon called acoustic radiation pressure [16]. A high sound pressure level is generated by focusing acoustic waves emanating from multiple sources, while constructive interference at the focus is achieved through the electronic control of the amplitudes and phases of the ultrasonic transducers. Modulating the focus (or foci) in time and/or space and at the right frequency causes perceptible vibrations on the skin, which has since then been termed as mid-air haptics [8], [17]; a technology commercialised by Ultrahaptics (now Ultraleap) since 2014. Applications of mid-air haptics include automotive human machine interfaces [11], wireless power transfer [18], digital signage [12], augmented, virtual, and mixed reality (AR/VR/MR) [19]–[21]. A comprehensive review article was recently published on this topic [10]. Other modulation and sound field synthesis techniques can make use of similar hardware to generate levitating holographic displays [22] and parametric directional audio [13].

The most commonly used hardware design of ultrasonic mid-air haptic technology is based on rectilinear arrays; a square grid of 200–300 ultrasonic transducers placed on a flat PCB. Larger or multiple array designs have also been constructed offering larger interaction regions [23]. Another approach to increasing interaction volume is to mount a standard-sized array on a robotic system that enables fast pan and tilt rotations [24], or indeed just mount it on the front of a VR headset [25]. Another hardware variant is that presented in [26] where a modified transducer layout was presented resembling a Fibonacci spiral arrangement, the effect of which is to reduce acoustic grating lobes (i.e., secondary unwanted focal points). All of these systems tend to suffer at varying degrees from a combination of drawbacks, including complex installation, large in size, complex electronic control, the need of a powerful host PC, high power requirements, and finally, high cost to build, assemble and deploy.

### B. Virtual buttons using haptic feedback

Virtual buttons have been investigated in multiple scenarios with different tactile feedback technologies. Nashel and Razzaque [27] proposed a vibration propagation technique to inform the button’s location, its functions, and its activation. When the path of the user’s finger is in contact with the area of the virtual button, the screen sends a pulse to indicate it is on top of a button. A different sensation is sent if the finger stays for a long period inside the button region. Kim and Lee [28] investigated the relation between haptic feedback in virtual

buttons based on the force graph of a physical button, and developed a method to provide feedback at multiple instances of the force graph.

Mid air haptic virtual buttons have been studied by Rümelin *et al.*, [29]. They investigated a single virtual button for a tap gesture interaction. They focused on short ultrasound stimuli and the variation of the frequency range. Marchal *et al.* [30] suggested adjusting the intensity of the button to emulate a change in its perceived stiffness. Another more sophisticated approach was developed by Ito *et al.* [31]. A mid-air dual-button was developed based on dividing the area of interaction in two layers. The top layer sends a sensation different than the bottom layer.

Other approaches include combining mid-air haptic displays with other technology. For instance, Ozkul *et al.* investigated complimenting mid-air haptic feedback with auditory stimuli for application to light switch button [32]. Finally, Freeman *et al.* suggested combining mid-air haptics with simple LED based visual feedforward, to guide hand movement during interaction (e.g., selection gesture) and then deliver haptic feedback [33].

## III. ULTRABUTTON OVERVIEW

The *UltraButton* combines visual, tactile and sound features embedded in and generated by a single device while using a minimal number of transducers and electronic complexity.

A single fixed focal point (FP) is generated in space, approximately 10 cm from the device centre axis, using a novel concentric ring arrangement of transducers. Then, a novel low-cost algorithm is applied for adding modulation onto the FP such that it is able to generate parametric audio sounds and haptic feedback. Finally, a proximity sensor is used to identify user input such as a hand-tap gesture and an LED strip is used to provide visual feedback and feedforward. All this is encapsulated in a single PCB plus a microcontroller logic board (the dimensions of the device are 150 mm in length and 230 mm in width) as shown in Figure 1. The transducers’ arrangement is contained inside a circular area of 120 mm diameter. Due to our minimalist approach, our prototype bill of materials (BOM) cost remains below \$200 which is one order of magnitude lower than the current mid-air haptic display commercially available.

### A. Ultrasound Transducer Arrangement

At the most basic level, to produce a focused ultrasonic field, one needs simply to drive a set of ultrasound transducers in such a way that every element contributes constructively at a specific point in space. Most ultrasound-based mid-air haptic displays rely on a collection of individually controlled ultrasound transducers. This allows for the flexibility to adjust the driving phase of each element so as to make the output constructive at any desired location but comes at the cost of complex and expensive driving electronics. To alleviate these problems, one can constrain the haptic point position and design a simpler ultrasound array accordingly. Instead of adjusting the driving phase electronically, we assume a single drive signal and adjust the location of the transducers

to achieve the desired constructive interference. The simplest way to achieve this is to assemble a concave-array where the array represents a section of a sphere of radius  $z$  and all the transducers on its surface are pointing inward. With such an arrangement, the transducers are all equidistant to the sphere centre and therefore interfere constructively at the focus location.

While such a concave-array can easily be produced using 3D printing and manually placing and connecting the transducers to the driving electronics [34], it remains impractical to integrate in other systems or to mass-produce.

Keeping the idea of a fixed haptic point, we suggest the use of a flat PCB with transducers arranged along concentric rings (see Fig. 2 (B)) such that a high pressure focus is formed above the centre of the rings (see Fig. 2 (A)). This transducer arrangement carries many simplifying benefits. First, since the distance to the desired central FP from each ring is the same, any one ring will naturally add constructively at the focus location. Second, it is possible to choose the ring radii in such a way that a common driving signal can be used for all rings.

The radius of each additional ring can be calculated by incrementing the distance from the focus to each ring by one ultrasound wavelength. Thus, additional rings at the correct incremental radii will add acoustic pressure to the FP. We note that the acoustic pressure contribution to the FP from a transducer in an outer ring is less than that from a more centrally located transducer due to the distance attenuation of the wave. However, outer rings will have more transducers and may therefore contribute more pressure to the FP in aggregate. The desired FP height  $z$  can be adjusted up or down by changing the radii of the rings. Transducer packing density on the PCB can be further increased by inverting the phase of every other ring by manually alternating the transducer polarity, thus effectively applying a  $\pi$  phase shift and allowing the distance of concentric rings to the FP to be separated by multiples of half a wavelength while still using the same driving signal. We thus separate transducers into two *groups*, each with a reversed polarity, such that alternating rings belong to the same group.

This can be understood geometrically in the diagram of Fig. 2 (A), whereby the radius of the  $n$ th concentric ring is defined by the inner most ring of transducers  $r_0$  and satisfies  $d_n - d_0 = (n - 1)\lambda/2$ , where  $d_n = \sqrt{z^2 + r_n^2}$  is the distance from the intended FP height  $z$  and the  $n$ th ring radius  $r_n$ . Rearranging the above equation for  $r_n$  we arrive at an expression for the appropriate radius which result in a single focus at  $z$

$$r_n = \sqrt{(\sqrt{z^2 + r_0^2} + (n - 1)\lambda/2)^2 - z^2}. \quad (1)$$

To decide on how many transducer rings to physically include in the design of the *UltraButton*, one needs to be able to calculate the pressure produced at the focus and ensure that it is high enough, e.g., 155 dB SPL. To do so, one can start by calculating the complex pressure  $P_t(p_z)$  at a point  $p_z$  due to a piston source emitter [35] at point  $p_t$  using

$$P_t(p_z) = \frac{P_{ref}}{d(p_z, p_t)} \frac{2J_1(ka \sin \theta_{zt})}{ka \sin \theta_{zt}} e^{i(\phi_t + k d(p_z, p_t))} \quad (2)$$

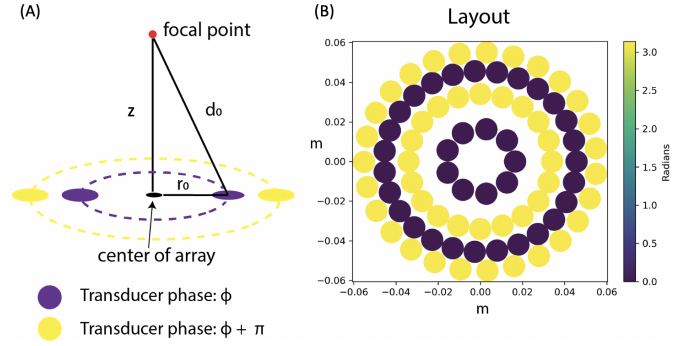


Fig. 2: (A) Schematic diagram showing how the radii of the two transducer groups are calculated to form concentric rings. (B) Transducer layout based on the concentric rings arrangement that will create a focus at  $z = 10$  cm. In this case, we have used  $n = 4$  rings with 9, 20, 27, and 27 transducers respectively, ( $T = 83$ , and  $r_0 = 2\lambda$ ).

where  $P_{ref}$  is a constant that is defined by transducer amplitude,  $d(x, y)$  is the Euclidean distance between points  $x$  and  $y$ , the transducer directivity function is defined by  $\frac{2 \cdot J_1(ka \sin \theta_{zt})}{ka \sin \theta_{zt}}$ , where  $J_1$  is the Bessel function of the first kind,  $k = 2\pi/\lambda$  is the wave-number,  $a$  is the transducer radius,  $\theta_{zt}$  is the polar angle between points  $p_z$  and  $p_t$ , and  $\phi_t$  is the initial phase of the transducer here set to 0 or  $\pi$  depending on the parity of  $n$ . Finally, to calculate the total pressure  $P(p_z)$  generated by the ring layout design (or any layout in fact) at the focus at  $p_z$ , one must compute the summation of the contribution of each transducer  $t \in [1, T]$  and take its absolute value  $P(p_z) = \left| \sum_{t=1}^T P_t(p_z) \right|$ .

To generate the acoustic fields and calculate  $P_T(p_z)$  we chose to use properties from the muRata MA40S4S transducer specifications sheet as these transducers can reliably produce a large amount of sound pressure (20 Pascals at a distance of 30 cm), operate at  $f_c = 40$  kHz ( $\lambda = 8.575$  mm), have a half-power beam-width of  $60^\circ$ , and a radius of  $a = 5$  mm. Finally, the transducer array design placement needs to also consider the physical radius of the transducers since this affects the number of transducers that can be packed in each ring, but also where other electronic components will be placed on the PCB such as a proximity sensor for detecting user input and LEDs for visual feedback. Using this approach, we found that the layout obtained in Figure 2 can produce a peak acoustic pressure of 2000 Pa, and averages to 152.75 dB SPL using Amplitude Modulation (AM), and 154 dB using 2 Frequency Modulation (2FM) defined in Sec. IV.

### B. Time of Flight Optical Sensor

To detect the presence and distance of the user's hand in front of the *UltraButton* device, we use the VL53L0X time-of-flight (ToF) proximity sensor by STMicroelectronics. The sensor contains a 940 nm laser source which is invisible and rated eye-safe, and a matching sensor that can measure the absolute range from 30 mm to 1 meter in its default mode of operation. For optical tracking, we placed the sensor at

the middle of the device, i.e., at the centre of the concentric rings and thus right under the mid-air haptic focus. The distance hand-device is computed by the microcontroller as the Euclidean distance between the device centre and the output of the VL53LOX sensor plus a small offset to account for the sensor height.

### C. LED Strip

To provide visual feedback before, during, or after user interactions with the *UltraButton* device, we have included a multi-colour LED strip soldered onto the PCB at the space between the first and second ring of transducers. This allows to provide the *UltraButton* users with additional visual information as discussed further down in Sec. VII.

### D. Microcontroller

To control the operations of the *UltraButton*, a driver board has been assembled composed of a Teensy 3.2 microcontroller that generates two digital periodic signals with the phase defined by the two groups of transducers. The amplifier driving the transducers is fixed at 20V and another 5V power supply is used to power the microcontroller, the proximity sensor and the LEDs. The micro-controller board does not need to be connected to a computer for sending phases to the array elements. This feature makes the device easy to use and integrate. The microcontroller makes use of 1 GPIO or 2 GPIOs to drive the transducer using the Amplitude Modulation or 2-Frequency Modulation, respectively. An additional 2 GPIOs are used to communicate with the proximity sensor and 1 GPIO is used to control the LED strip. Therefore, out of the 23 GPIOs available on Teensy 3.2, up to 18 of them are unused. The extra GPIOs can be used to connect to additional peripherals, including communication peripherals such as Bluetooth dongle. This last possibility is explored further in the application section VII.

## IV. MODULATION TECHNIQUES

In this section, we describe two algorithms producing a haptically perceivable FP at a short distance above the device, namely, Amplitude Modulation (AM) and Two Frequency Modulation (2FM). We then describe how to modulate an audio signal to produce directional audio, and discuss audible noise artefacts and health & safety considerations associated with the *UltraButton*.

### A. Amplitude Modulation

Amplitude Modulation (AM) is the most commonly used technique for mid-air tactile display and for generating parametric audio [9]. It modulates the ultrasound pressure intensity between 0 and 1 at a given periodic frequency while keeping the FP position fixed in space. In 3 (A), one can observe the simplicity of this technique and how a phase shift is applied to the carrier frequency at the different groups of transducers.

The AM driving technique is based on the superposition of two waves, the carrier signal which is a high frequency signal of, e.g.,  $f_c = 40$  kHz in our case, and the modulating signal which is around, e.g.,  $f_m = 200$  Hz for mid-air haptics, and

may vary for parametric audio. The equations characterising the AM technique are thus:

$$\begin{aligned} Y_c &= A_c \sin(2\pi f_c t) \\ Y_m &= \frac{A_m}{2} (1 - \cos(2\pi f_m t)) \\ Y_{AM} &= Y_c \times Y_m = \frac{A_c A_m}{4} [2 \sin(2\pi f_c t) \\ &\quad - \sin(2\pi(f_c + f_m)t) + \sin(2\pi(f_c - f_m)t)] \end{aligned} \quad (3)$$

where  $A_m \in [0, 1]$  and  $A_c$  are the amplitudes of the modulating carrier signals, respectively. The Root-Mean-Square of the amplitude modulated signal  $Y_{AM}$  is equal to  $\sqrt{\frac{3}{16} \frac{A_c A_m}{4}} \approx 0.43 \frac{A_c A_m}{4}$ .

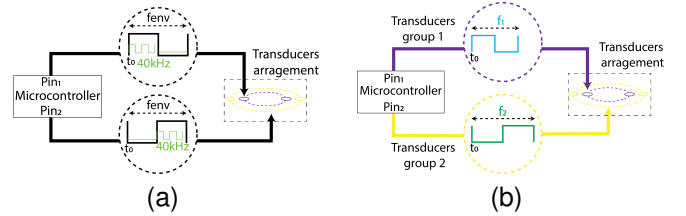


Fig. 3: (a) AM algorithm: A single signal drives both groups of transducers. Since the two groups are reverse polarised (shown in yellow and purple), a  $\pi$  phase shift is naturally applied to the carrier frequency to produce a focus. The focus is then modulated by an envelope frequency (e.g., 200 Hz for haptics). (b) 2FM algorithm: Slightly different signals are sent to each transducer group.

### B. Two Frequency Modulation

Using two frequency modulation (2FM) is an alternative and novel method that can generate a modulated FP that is haptically perceivable to the skin receptors. The 2FM technique is based on the sum of two waves with nearby but different carrier frequencies  $f_1 = f_c + \delta f$  and  $f_2 = f_c - \delta f$ . When these two carriers interfere, a “beat frequency” effect develops and produces the frequency  $f_{beat} = |f_1 - f_2| = 2\delta f$  (see Figure 3 (B)). By setting the beat frequency at the same value as the modulation frequency in the AM technique (i.e.,  $f_m = 2\delta f$ ), we modulate the FP amplitude in a similar way than with the AM technique, which will “feel” the same to the user (see section V-B). We note that beat frequencies have been extensively studied and used in a number of wave applications, however, this is the first time they are used for mid-air haptics. The equations characterising the 2FM technique are thus:

$$\begin{aligned} Y_1 &= \frac{A_c}{2} \sin(2\pi f_1 t) \\ Y_2 &= \frac{A_c}{2} \sin(2\pi f_2 t) \\ Y_{2FM} &= Y_1 + Y_2 = \frac{A_c}{2} (\sin(2\pi f_1 t) + \sin(2\pi f_2 t)) \end{aligned} \quad (4)$$

where  $f_1$  is the signal frequency of the first group and  $f_2$  is the signal frequency of the second group, which for *UltraButton* is



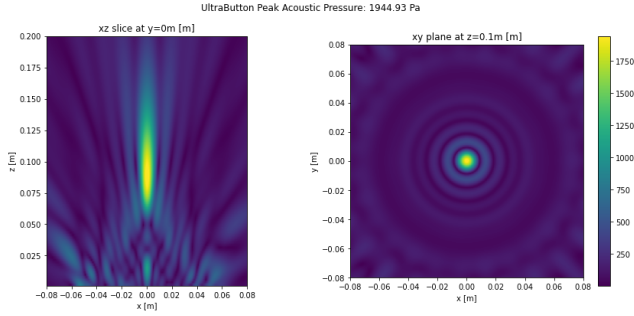


Fig. 4: Simulated acoustic field pressure with a focus at  $z = 10$  cm. On the left is a cross-section from the device side, while on the right is a cross-section along the  $z = 10$  cm plane.

placed on different rings on the PCB as described previously. The Root-Mean-Square of the amplitude modulated signal  $Y_{2FM}$  is equal to  $\frac{1}{2} \frac{A_c}{2} = \frac{A_c}{4}$ . Therefore, to obtain the equivalent AM frequency of 200 Hz at the FP, one should choose  $f_1 = 40100$  and  $f_2 = 39900$  when using 40 kHz resonant transducers like the MA40S4S. Note that both these frequencies are close enough to the resonant frequency (less than 1% variation) therefore minimising any loss in output and are compatible with the transducer ring arrangement. After submission of this paper for review, Mizutani et al. [36] suggested driving multiple arrays at different frequencies to produce a haptic sensation. We remark that *UltraButton* leverages multiple frequency modulation to produce a haptic sensation at the circuit level of the system (see Figure 3b).

Finally, we note that the 2FM scheme drives each transducer at full power resulting in maximal utilization of each transducer's output, unlike the AM scheme which has an effective 50% duty cycle (see Figure 5 (C)). However, as each transducer is at full-blast, a continuous and prolonged mid-air haptic FP might result in self-heating of the transducers. This should be less of a problem at low duty-cycles, e.g., for a mid-air button-like tap where a short burst of high intensity pressure is generated.

### C. Haptic Feedback

The acoustic radiation force produced by a FP of 155 dB SPL produces around  $1\mu\text{m}$  of skin indentation [37]. For the FP to result in a tactile perceptible vibrational effect, a modulated signal between 5 Hz and 1000 Hz is necessary, however further restricting this range to 50-300 Hz is more likely to be felt [8], [38], with lower/higher frequencies corresponding to rougher/smooth tactile sensations [39]. As discussed above, the *UltraButton* can generate sufficient acoustic radiation force and a perceptible tactile modulation at the FP using either the AM or the 2FM scheme. The acoustic field generated by the device is shown in Figure 4. The circular symmetry of the transducer layout manifests itself as a signature in the acoustic field (see right picture in Figure 4), while the high acoustic pressures that surround the FP are an unwanted and unavoidable side-effects of the *UltraButton* transducer layout, however, are below our tactile perception threshold.

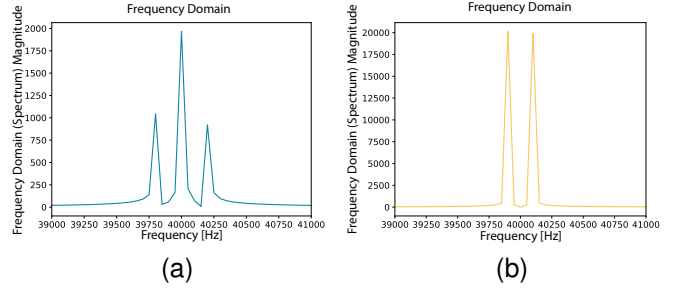


Fig. 5: Fourier spectrum of AM (a) and 2FM (b) and their temporal variation modulated at 200 Hz (c).

The pressure field however is not enough to explain if a focus is perceivable by a human hand. To see this, one needs to also simulate the temporal variation of pressures due to  $Y_{AM}$  and  $Y_{2FM}$  along with their Fourier spectrum as shown in 5. Note that the Fourier spectrum of the two modulation schemes are quite different with 2FM having a more efficient energy distribution. Despite this, their resulting acoustic fields and the temporal pressure variations are indeed very similar. Although a formal user study is yet to be conducted, the two modulation schemes feel very similar, if not identical. In section V we will show that both algorithms can be perceived as equally strong for all the test forces.

### D. Audible Sounds and Noise

Parametric audio is the well-known phenomenon whereby audible sound is produced from ultrasound through nonlinear mixing in the air [40]–[42]. Westerveldt shows that, to first order, the mixing sound generated by two coincident sound waves is proportional to the product of their pressures and the square of their difference frequency [40]. This is a volumetric effect whereby the larger the volume of air with different frequencies traveling co-linearly in it, the more mixing sound will be produced. Together, this yields the directed-audio effect from ultrasonic end-fire arrays modulated with an audio signal [42]. In that case, a large area of transducers is all producing the same AM content, producing a multi-frequency wavefront which mixes as it propagates. Since the end-fire array is typically large compared to the wavelength, the ultrasound remains collimated for long distances.

The *UltraButton* has enough acoustic pressure to generate parametric audio which starts to occur at approximately 135 dB PSP. By modulating the transducers with an audio signal (either with amplitude modulation or a more sophisticated single sideband technique), it can act as a small speaker. Because the array is configured to focus, rather than create a collimated beam like an end-fire array, it will not have the same beam-like properties but can still produce a noticeable amount of audio localised above the device as if emanating from a point source. The AM audible signal overlaid onto the ultrasound carrier can produce a variety of sounds, beeps, clicks, voices and even music, however, the quality tends to deteriorate and distort for low-pitch sounds.

More important than its ability to create audible sound is the system’s ability to prevent audible sound while generating mid-air haptics. Rapid changes to the acoustic field can cause unwanted audible noise [43]. This can be understood as a product of the increased efficiency of nonlinear mixing at higher frequencies and rapid changes that inexorably include higher modulation frequencies. Since the *UltraButton* only consists of a single driving signal, optimizing that signal to be as smooth as possible comes at a lower cost than for a similar effort in an individually-driven phased array. This can be done by increasing the accuracy (bit-depth) of a PWM driving signal or using an analog system. For the prototype presented here, a simple M4 microcontroller is already able to generate a PWM signal with 10-bits of resolution.

The 2FM scheme produces even further reduction of unwanted audible noise by reducing the volume of space where multiple frequencies are co-linear and able to mix. In the 2FM scheme, any one transducer is only producing a single frequency of ultrasound and therefore, alone, is not producing any parametric audio. Only as the wavefronts arrive at the focus is there any possibility of nonlinear mixing. Even then, this volume is limited in size as the waves quickly converge, focus, and then diverge. The net result is that the 2FM scheme produces noticeably less audio noise (usually heard as a small buzz) when compared to the AM scheme while producing nearly identical haptic feel.

### E. Safety in mid-air haptic feedback

When designing mid-air haptics one also needs to consider safety guidelines and best practices relating to high intensity ultrasound and potential hearing damage. High intensity ultrasonic arrays of transducers working at 40 kHz have been studied in several papers [44], [45] to examine the acoustic energy exposure levels experienced by a user during interaction with a mid-air haptic FP. These studies note that the pressure away from the location of the FP drops rapidly, typically by 20+ dB by the time it reaches the user’s head. Furthermore they show that exposure to up to 120dB SPL at the ear, over a period of 5 to 10 minutes induces no change in hearing sensitivity. Additionally, international guideline provided by the ACGIH and adopted by the U.S. Occupational Safety and Health Administration (OSHA) recommends a maximum limit of 145dB at the ear. *UltraButton* produces up to 154dB SPL at the FP, but this will drop to 134dB SPL and more by

the time it reaches the user’s ear. Furthermore, *UltraButton*’s ultrasound transducers are only activated for a short amount of time (150ms click burst) and the proximity sensor controls when the device is on. Hence, we can affirm that *UltraButton* is safe for the user’s hearing.

## V. EVALUATION OF HAPTIC FEEDBACK

The *UltraButton* relies on the premise that the novel transducer spatial arrangement generates comparable acoustic pressure at the focal point (FP) as other ultrasound mid-air haptic devices. Hence, the force applied to the user’s skin should be comparable, inducing haptic stimuli of equivalent perceptual strength. To test this premise, we have evaluated the haptic feedback of *UltraButton* against that of a commercially available ultrasound mid-air haptic device, namely a Stratos Explore from Ultraleap Ltd. First, we registered the force generated by the FP generated by the *UltraButton* and the Stratos Explore development kit across a range of intensities input using a precision scale microbalance. Then, we ran a quantitative user study in which participants rated the perceived strength of the FP produced by either devices at various force levels.

### A. Focal Point Generated Force

In this experiment, we measured the force generated at the FP by *UltraButton* and Stratos Explore development kit consisting of 256 transducers (16x16 rectilinear phased array) using a precision scale (KERN PCB 2500-2). To isolate the FP acoustic pressure from the ambient acoustic pressure, we positioned a foam board with a circular hole of  $\sim 20$  mm diameter a few centimetres above the precision scale. The foam board was fixed and suspended (non grounded) just over the balance scale thus blocking any acoustic force, except that of the FP. Further, we placed a small cylindrical pillar of 20 mm diameter on top of the precision scale, with its top surface aligned with the foam board. The ultrasound devices were positioned upside-down (transducers facing down) 10 cm above the foam board and were aligned with the pillar so that the FP centre matched the pillar surface centre. The obtained setup is represented in Figure 6a.

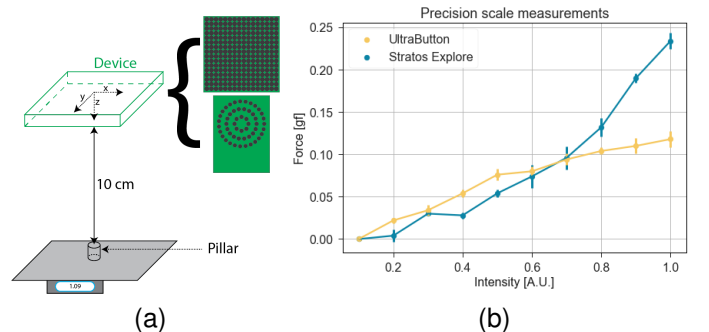


Fig. 6: a) Setup used to measure the FP force of the two ultrasonic mid-air haptic devices. b) Plot of the force measured as a function of the FP intensity for the two ultrasonic devices.

Then, we measured the force generated by each device, for intensity inputs ranging from 0.1 to 1 by step of 0.1. The Stratos Explore device generated an AM point at 200 Hz, while the *UltraButton* generated a 2FM point at 200 Hz. Each measurement was repeated five times and averaged before being reported in Figure 6b. The results show that both devices generate comparable forces up to intensity 0.8. This was expected as the higher number of transducers in the Stratos Explore enables the creation of focal points at a much higher acoustic pressure.

### B. User Study

Based on previous works [46], [47], the forces showed in Figure 6b are above the tactile perception threshold for ultrasound mid-air haptics when  $\sim 0.04$  gf. However, to be sure that participants could perceive the haptic stimuli from the two devices, in our user study we chose to use forces values well above that threshold but lower than the point where the two curves in Fig. 6b diverge. We therefore restricted the study to forces ranging from 0.08 gf to 0.12 gf, with a step of 0.01 gf. In our studies, we compared the perceived strength of 2FM haptics using *UltraButton*, and AM haptics using Stratos Explore. However, since the 2FM technique has a slightly different envelope compared to the traditional AM technique (as discussed in Sec. IV-C) potentially affecting the tactile perception of the generated haptics, we used results from Figure 6b to adjust the output intensities so that an equivalent force is produced between the two devices during the comparison. Specifically, for *UltraButton* we used the forced measured on the precision balance as they were already matching the range of the chosen forces, whilst for the Stratos Explore, we fitted the data obtained from the precision balance measurements to a quadratic model ( $R^2 = .98$ ) and predicted the intensity values needed to produce the test forces. Finally, we ran a magnitude estimation task comparing the perceptual performance of the two ultrasound devices.

#### 1) Participants

A total of 23 participants took part in this study (age  $\mu = 31.6$ ,  $\sigma = \pm 4.6$ ). They had normal or glasses/lens corrected vision and no history of neurological or psychological disorders. Upon arrival, participants were asked to read the information sheet and sign a consent form before the task was explained to them. Further, all the procedural steps were indicated on the experiment GUI.

#### 2) Procedure

The procedure is summarised in Figure 7. Participants sat in front of the setup illustrated in Figure 7 (A) with their left hand facing downwards on a dedicated hole (gap). Beneath it, the two devices, *UltraButton* and Stratos Explore were positioned on a moving platform that was hidden from the participants. Participants were also required to wear headphones playing white noise to isolate devices and environment noises. Hence, participants could not see nor hear the mid-air haptic devices or the moving plate while operating. We followed a magnitude estimation task procedure in which we presented pairs of stimuli composed of a fixed reference and a comparison stimulus. The *reference* was rendered by the Stratos Explore

and was set at 0.1 gf which corresponds to the middle value for the range of test forces chosen for this experiment - 0.08 to 0.12 gf. The *comparison* stimulus contained each time, one of the five forces to rate for *UltraButton* and the Stratos Explore, and was presented in a randomised order. In total, we tested five forces for each of the two ultrasonic devices corresponding to 0.08, 0.09, 0.1, 0.11, and 0.12 gf. Prior to the experimental phase, participants were informed that the reference stimulus had a fixed arbitrary value of 100. After the reference stimulus, a second stimulus (comparison) was delivered; participants were requested to rate the comparison stimulus in contrast with the reference one. Therefore, if the comparison stimulus was felt as twice stronger, a value of 200 was inserted. If it was perceived as half stronger, a value of 50 was inserted, etc. Before delivering each of the haptic stimuli for one second (i.e., reference and comparison), participants could hear a 500 ms “beep” sound from their earphones to focus their attention. We employed a within-participant design with three repeated measurements for each force for a total of  $5 \text{ (forces)} \times 2 \text{ (devices)} \times 3 \text{ (repetitions)} = 30$  stimuli.

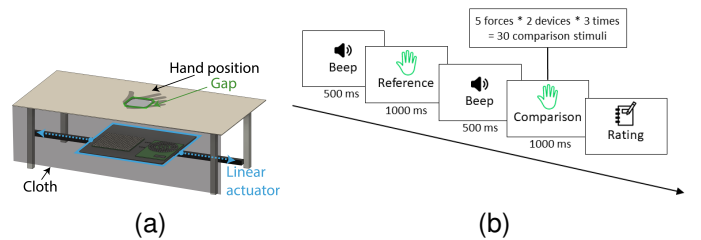


Fig. 7: a) Experimental setup. Participants placed their left hand onto the gap. A linear actuator was positioned on one of the two ultrasound devices under participant’s palm. The setup was hidden by a black cloth. b) Experimental procedure used for the user study. Participants could feel a first reference stimulus, then there was a second stimulus that they had to rate in comparison to the reference.

#### 3) Results

Figure 8 shows a box plot for the ratings of the five forces tested, colour-coded and grouped by the two devices. A Shapiro-Wilk test indicated that our data was likely to significantly deviate from a normal distribution ( $p < 0.001$ ).

Then, we carried out multiple Wilcoxon tests to explore the differences in the strength of the tested forces between *UltraButton* and the Stratos Explore device. Each level of the variable force is summarized in Table I. For *UltraButton* force levels, there were five different force combinations that were differently perceived by the participants. Moreover, for the Stratos Explore, there is a non-significant difference between forces 0.11 and 0.12 gf ( $p = 0.061$ ).

All the comparisons appeared to be statistically not significant ( $p > 0.05$ ). In other words, participants perceived the stimuli of the two devices as equally strong for all the tested forces. Further, to explore if participants were able to feel a change between the different force levels within the same device, we ran two Friedman tests, one for *UltraButton* and one for the Stratos Explore. Both tests confirmed a statistical

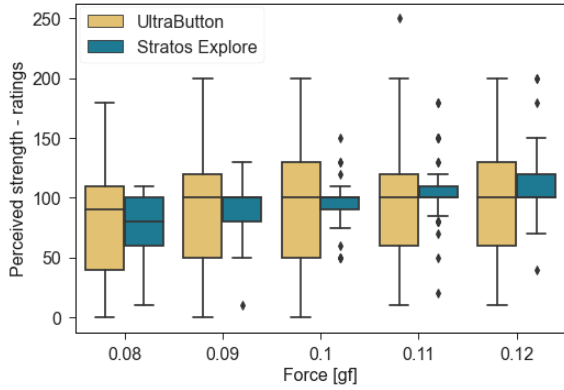


Fig. 8: Box plot showing participants’ ratings divided per test forces. In yellow, the ratings for the *UltraButton* device, in green, the ratings for the *Stratos Explore*.

difference of the perceived strength between the different force levels ( $p < 0.001$ ). The data shows that *UltraButton* ratings have a significantly higher variance than *Explore Stratos*. This perception can be caused by differences in the FP rendered of these devices and then influence the user’s perceived force.

Forces (gf)	0.08	0.09	0.10	0.11	0.12
0.08	X				
0.09	0.05	X			
0.10	<0.001	0.090	X		
0.11	0.001	0.201	0.799	X	
0.12	<0.001	0.007	0.345	0.213	X

TABLE I: Wilcoxon test results for each pair of tested force for the *UltraButton* device. The cells report the p value for each test. In green, the significant differences. In red, the non-significant differences.

## VI. EVALUATION OF ULTRABUTTON AS A SYSTEM

We performed a second experiment to investigate the functionality of the *UltraButton* as an interactive system composed of an array of transducers, a ToF sensor, and an LED strip. For our evaluation, we selected 12 mid-air buttons with varying height threshold (four heights - from 10 to 150 mm) and haptic burst duration (three values - from 50 to 300 ms). In all cases, the LEDs were flashing for 100 ms. Beyond usability, we aimed at understanding user preferences across these two calibration parameters. We chose a limited set of values to avoid the participants to get used to the task and repeat automatically the same push action for all the buttons. We chose easily differentiable feedback activation onset heights, from near to far the FP, with click-like haptics duration (50 ms), a duration equal to the flashing LEDs (100 ms), and a longer one (300 ms). Further optimization is possible however is beyond the scope of this paper.

### 1) Participants

Ten participants were recruited (age  $\mu = 31.7$ ,  $\sigma = \pm 5.37$ ). Upon arrival, they were asked to read and sign a consent form before the experiment task was explained to them.

### 2) Setup and Procedure

A laptop and the *UltraButton* were placed on a desk in a quiet room along with a chair for participants to sit during the study. No headphones were used, as the FP sound was not audible (see IV-D). All participants were right-handed, by chance, so the device was placed on the laptop’s right side. The laptop screen displayed the task instructions and a trial counter from 1 to 12 for each block. The user could have a short break in between blocks. Participants were instructed to press the mid-air button located just above the *UltraButton* just as if they were approaching a physical button and to freely move their right hand above the *UltraButton* system as they thought best. The ToF would register their action and would then provide haptic and visual feedback (no audio). When they thought they successfully pushed the mid-air button, they were instructed to press the keyboard space-bar to proceed to the next trial. The laptop played a ‘beep’ sound at the beginning of each trial, after which the participant could start performing the push action. Following the study, the researcher performed a semi-structured interview to investigate the participants’ experience with the system. The whole procedure lasted approximately 15 min per participant. A simple interaction diagram is shown in Fig. 10.

### 3) Study Parameters

The participants tested 12 different realizations of the *UltraButton*. In all cases, the haptic FP location was fixed at 100 mm (the algorithm sends the same phase delay per concentric ring, which will arrive at 100 mm at the centre of the device creating a 200 Hz modulation) and would activate as soon as the ToF sensor detects the user’s hand crossing the feedback onset height threshold. Each *UltraButton* realization had a different haptic feedback duration (50, 100, and 300 ms) and a different feedback activation onset height (10, 60, 100, and 150 mm above the FP location). All these combinations were tested in random order and repeated three times, giving 36 trials per participant.

### 4) Results

We analysed participants’ pushing and realising behaviour by focusing on the minimum distance reached by their hand while pushing the buttons and looking at the time spent completing the interaction. We grouped the participants’ behaviour by the four different feedback activation onset heights tested. The ToF times-series data were pre-processed to filter any sensor anomaly and then fitted to a parabolic curve. Finally, data were averaged over the 10 participants for each of the four feedback activation onset heights. Note that the raw data were already very close to a parabola. In Fig. 9, we show the resulting three parabolas for each haptic duration time and each of the four different feedback activation onset heights.

At first visual inspection of Figure 9, we observe that the haptic duration time did not have a significant influence on the minimum distance reached by the participants’ hand when pushing the mid-air buttons, since all curves in each sub-figure reach a similar lowest point. In addition, there is only a small proportional trend between haptics duration and task time. To test that, we performed an ANOVA repeated measures within each group which did not highlight any significant differences,



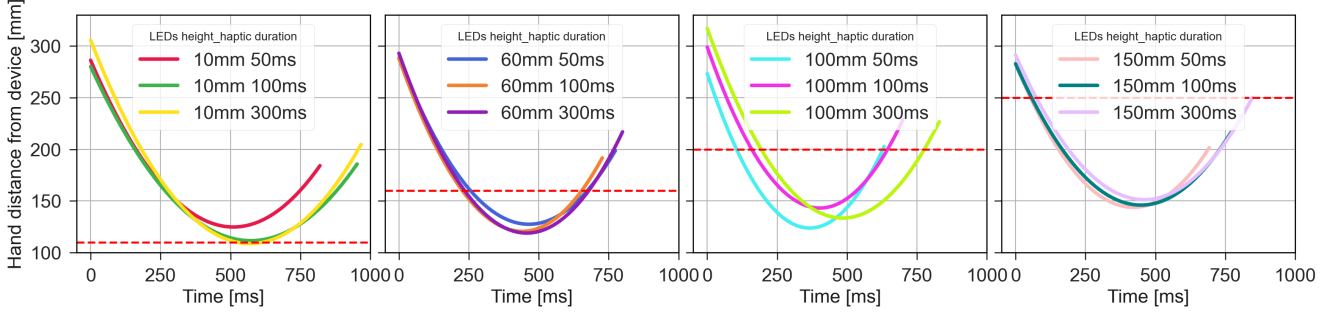


Fig. 9: Participants’ behaviour when pressing the 12 buttons grouped by the four LEDs activation heights tested. The red dashed line represents the LED activation height. Overall, it appears the participants’ hand reached for the haptic sensation fixed at 100 mm.

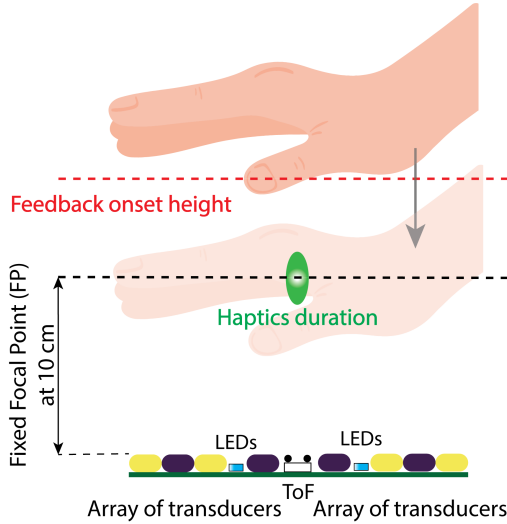


Fig. 10: Experimental setup. We designed 12 buttons which combined four feedback activation onset heights ( $Feedback - Onset_{height} \in 10 \text{ mm}, 60 \text{ mm}, 100 \text{ mm}, 150 \text{ mm}$ ) from the distance of the FP and three haptic sensation times ( $haptic_{time} \in 50 \text{ ms}, 100 \text{ ms}, 300 \text{ ms}$ ). In the experiment, participants had to perform a push action in mid-air. The haptic sensation was always at the same height (100 mm) from the centre of the device.

neither for the minimum distance reached by participants’ hand, nor for the time to complete the task ( $p > 0.05$ ).

Further, we considered differences between the feedback activation onset height and the 12 test variants of the *UltraButton*. Regarding the minimum distance from the device reached by participants’ hand, we observed significant statistical differences for both the minimum distance ( $\chi^2 = 19.320$ ,  $p < 0.001$ ) and the task time ( $\chi^2 = 8.040$ ,  $p = 0.04$ ). We have found differences between the minimum distance reached by participants’ hand and the buttons whose feedback activation onset height was set to 10 vs 100, 10 vs 150, and 60 vs 150 mm, with the smaller feedback activation height leading to hand minimum distance from the device. The only significant difference time-wise was between the button whose feedback was activated at 10 vs 100 mm. Overall, we can observe how

participants, despite the feedback being activated at different heights, tended to continue the hand movement until being near the FP location at 100 mm, even if the LEDs had already turned off by that point. We note that while the FP centre is at  $z = 100 \text{ mm}$ , the high intensity acoustic field of the FP stretches up to 130-150 mm as seen in the simulations of Figure 4. Indeed, the haptics was perceivable at that range but felt stronger closer to the FP centre. Thus, we argue that the haptics played a more significant role in the participant’s hand motion than the LEDs.

Finally, we would like to summarise the most relevant points extracted from the interviews with the participants. Nine participants reported preferring the button whose feedback activation onset height and haptics were at 10 cm from the device. This confirms and explains the behaviour we observed in the previous paragraph (i.e., the participants prefer to feel stronger haptics and be at a more natural distance from the system). Eight participants reported preferring longer haptic sensations. That, “*makes the sensation more perceivable, and it provides a higher degree of confidence in understanding that the action was successful*”. All the participants mentioned they relied equally on the LEDs and the haptics, even if five of them reported that when they could not feel the haptics, they felt the action was “*weird*” as if they did not complete the task successfully. All the participants thought they would use the mid-air haptic button in a real scenario, if available, mainly motivated by hygienic reasons. Some participants commented they prefer a more refined design or dev kit rather than a research prototype. We also noticed an interesting effect where three participants mentioned that they perceived the LEDs duration as varying with the haptics duration, indicating a prevailing effect of haptics on visual time perception.

## VII. INTERACTIONS AND APPLICATIONS

The *UltraButton* is a minimalist touchless button device that supports a plethora of multimodal interactions through its input and output sensors and microcontroller connectivity. Namely, the present device detects simple gesture input such as a tap and double-tap using the onboard proximity sensor. Visual, audible, and haptic feedback can be pre-programmed and flashed onto the microcontroller and threshold or variability triggered by such user gesture inputs, or can be time-delayed

accordingly. The proximity sensor can also use the estimated hand-to-device distance to provide feedforward information (e.g., to guide, prime, or inform the interaction) using one or many of the available modalities, which can be multiplexed in time to create a sequence of interactive experiences. Note that audio and haptics cannot be triggered simultaneously. An example of a touchless multimodal button tap interaction is shown in Figure 11.

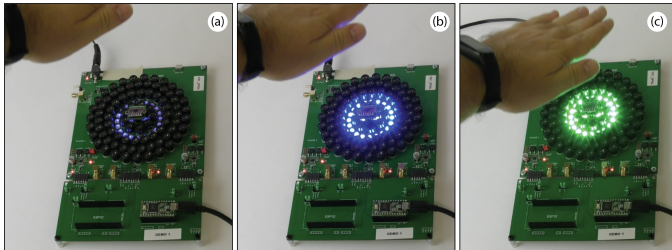


Fig. 11: (a) Example of a touchless button click interaction with visual feedforward. (b) Visual plus haptic feedback at the beginning of a tap gesture. (c) Visual plus audio feedback at the end of the tap gesture.

Each of the three modalities available to the *UltraButton* (visual, audio, and haptics) has a rich and easy to understand design space. The LEDs can change colour (Red, Green, Blue), adjust their brightness, and can turn on and off independently. Audible sounds (beeps, clicks, voice, and music) can be generated using parametric audio modulation techniques – the sound quality deteriorates for low-pitch sounds. Finally, the fixed in space mid-air haptic FP can vary its intensity or blink on/off at different rates to emulate a button click’s temporal force profile (usually lasting about 100 ms) or indicate some notification of functionality. The possible combinations are therefore many, providing a wide design space for user experience designers to tailor to the applications at hand.

The *UltraButton* can find applications in various settings. This is facilitated by its small footprint ( $\sim 100 \text{ cm}^2$ ), its extensive microcontroller input/output connectivity, its low cost ( $\sim \$100 - 200$  depending on bulk order), and its low power requirements ( $\sim 25$  Watts). The *UltraButton* can be battery-powered for mobile applications, connected to the internet through a WiFi or Bluetooth dongle, or can be chained to many *UltraButton* devices to form an *UltraPanel*. With public touch surfaces such as touchscreens, elevator panels, ATMs, and pedestrian call buttons under scrutiny for being pathogen spreading hubs [3], [48], [49], *UltraButton* offers a compelling alternative solution.

Multiple *UltraButton* devices can be assembled and designed to be integrated into control panels, for example, an elevator panel as in Figure 1 (C). The interaction design of such interfaces must be carefully thought of, designed, and tested. As a proof-of-concept for the elevator example, one could consider using just two *UltraButtons* for the up and down call buttons, with easily recognisable visuals and sounds to assist in the interaction. Different colours can be used for the up and down buttons; they could change before and after a tap interaction and indicate the current floor or the desired direction of travel (e.g., down). Simple beep or click

sounds can be generated just after the interaction while haptic feedback can be presented during the interaction on the user’s palm or fingertip. A demo prototype of an accessible elevator using commercial mid-air haptic devices was proposed by [50]. Similar setups can be assembled for light switches, push-to-exit doors, water fountains, sanitary paper, liquid soap dispensers, and other simple interfaces in public spaces.

Various fun game applications can also be thought up and created with *UltraButton*, before being deployed in location-based entertainment (LBE) venues. For instance, a touchless Whac-A-Mole game could be created using multiple *UltraButtons* arranged in a grid and made to light up at random, to be tapped/whacked in mid-air; as we discovered in VI changing the activation of LED at different times will change the perception of the users and miss the target making the game more enjoyable. Such a solution would support widespread public usage without worrying about cross-user contamination and spreading disease.

Finally, the multimodal feedforward and feedback capabilities afforded by the *UltraButton* can guide and help keep a user’s hand steady at a set mid-air location and pose while image authentication algorithms run in the background [51].

## VIII. CONCLUSION

We have presented *UltraButton*, a minimalist touchless multimodal haptic button. Our prototype implementation (see Figure 1 (A)) utilises 83 ultrasound transducers and produces perceivable mid-air haptic feedback and sound source at 10 cm above the device. *UltraButton* also provides visual feedback through 20 LEDs soldered onto a single PCB alongside the ultrasound transducers and a proximity sensor. The whole system is controlled via a microcontroller and makes use of low complexity commodity electronics resulting in a total bill of materials (BOM) that costs under \$200, unlike full-blown mid-air haptic and multimodal displays which utilise phased ultrasound arrays that can cost a lot more to manufacture. Its core enabling feature is its ability to deliver simple mid-air haptic sensations in addition to audible feedback such as a button “click” at short distances from the device. The user can trigger them via basic gesture inputs detected by the onboard proximity sensor. To that end, we have described a simple but novel ultrasound modulation driver signal (2FM) capable of inducing mid-air tactile sensations and one audio modulation technique for generating directional sound playback.

To evaluate *UltraButton*, we ran two formal experiments comparing the haptic feedback (i.e., the acoustic radiation force of a focal point at 10 cm above the device surface) generated by *UltraButton* and a commercially available mid-air haptic display (i.e., Stratos Explore from Ultraleap Ltd.). First, we used a precision scale to measure the acoustic radiation pressure generated at the FP and revealed that *UltraButton* can generate forces well above the perception’s threshold and comparable with the Stratos Explore device. Secondly, we designed a user study exploiting a magnitude estimation task procedure to evaluate the perceived strength of the mid-air haptic feedback generated with our novel 2FM algorithm using *UltraButton* against the feedback generated with the more

traditional AM algorithm using the Stratos Explore device. The study showed that at equal force outputs, there were no statistically significant differences between the perceived haptic effect of the two algorithms and devices, and therefore both algorithms produce haptic feedback that is perceived with equal strength.

Finally, a third user study was designed to evaluate the whole system by creating 12 different mid-air buttons. This set of buttons varied the activation of LEDs at different heights and the duration of the haptic sensation. We found that visuo-haptic feedback influenced the hand trajectory during button press gestures. The post-study interview revealed a preference for mid-air haptic and LED activation height to be congruent when the activation height is closest to the FP location.

*UltraButton* offers a low-cost, low-footprint, yet versatile solution for enabling haptic feedback on touchless interfaces. The multimodality of the *UltraButton* along with its connectivity, feedforward, feedback, and multiplexing capability options presents HCI and UX designers with a rich but simple tool to understand and experiment with to create novel touchless interfaces and applications. In our paper, we discussed some ideas such as an elevator panel (see Figure 1 (C)), games, and hygienic public interfaces. We hope that this work can inspire and guide future studies, applications, integrations, and implementations of touchless multimodal interfaces. Despite this, it should be noted that many simplifying trade-offs had to be made to reach *UltraButton*, such as the versatility and range afforded by phased array solutions that can generate multiple FPs at multiple locations in 3D space.

Finally, we would like to stress that each design step of our approach (i.e., layout and driving signal) has been described thoroughly in this paper and uses solely off-the-shelf electronics, hence facilitating the reproduction and adaptation of *UltraButton*-like devices by the community. Therefore, we hope that our studies will pave the way to a whole new ecosystem of *UltraButton*-like devices and their integration into many multimodal mid-air haptic interfaces.

#### ACKNOWLEDGMENTS

This research is funded by the European Union's Horizon 2020 research and innovation programme, grant No 737087 (LEVITATE) and No 101017746 (TOUCHLESS).

#### REFERENCES

- [1] N. Zhang and Y. Li, "Transmission of influenza a in a student office based on realistic person-to-person contact and surface touch behaviour," *International journal of environmental research and public health*, vol. 15, no. 8, p. 1699, 2018.
- [2] C. P. Gerba, A. L. Wuollet, P. Raisanen, and G. U. Lopez, "Bacterial contamination of computer touch screens," *American journal of infection control*, vol. 44, no. 3, pp. 358–360, 2016.
- [3] N. Ikonen, C. Savolainen-Kopra, J. E. Enstone, I. Kulmala, P. Pasanen, A. Salmela, S. Salo, J. S. Nguyen-Van-Tam, and P. Ruutu, "Deposition of respiratory virus pathogens on frequently touched surfaces at airports," *BMC infectious diseases*, vol. 18, no. 1, pp. 1–7, 2018.
- [4] K. Okerefor, I. Ekong, I. O. Markson, and K. Enwere, "Fingerprint biometric system hygiene and the risk of covid-19 transmission," *JMIR Biomedical Engineering*, vol. 5, no. 1, p. e19623, 2020.
- [5] F. Marzoli, A. Bortolami, A. Pezzuto, E. Mazzetto, R. Piro, C. Terregino, F. Bonfante, and S. Belluco, "A systematic review of human coronaviruses survival on environmental surfaces," *Science of The Total Environment*, p. 146191, 2021.
- [6] S. Villarreal-Narvaez, J. Vanderdonckt, R.-D. Vatavu, and J. O. Wobbrock, "A systematic review of gesture elicitation studies: What can we learn from 216 studies?" in *Proceedings of the 2020 ACM Designing Interactive Systems Conference*, 2020, pp. 855–872.
- [7] R. Walter, G. Bailly, and J. Müller, "Strikeapeose: revealing mid-air gestures on public displays," in *Proceedings of the SIGCHI Conference on Human Factors in Computing Systems*, 2013, pp. 841–850.
- [8] T. Carter, S. A. Seah, B. Long, B. Drinkwater, and S. Subramanian, "Ultrahaptics: Multi-point mid-air haptic feedback for touch surfaces," in *Proceedings of the 26th Annual ACM Symposium on User Interface Software and Technology*, ser. UIST '13. New York, NY, USA: Association for Computing Machinery, 2013, p. 505–514. [Online]. Available: <https://doi.org/10.1145/2501988.2502018>
- [9] F. J. Pompei, "Sound from ultrasound: The parametric array as an audible sound source," Ph.D. dissertation, Massachusetts Institute of Technology, 2002.
- [10] I. Rakkolainen, E. Freeman, A. Sand, R. Raisamo, and S. Brewster, "A survey of mid-air ultrasound haptics and its applications," *IEEE Transactions on Haptics*, 2020.
- [11] K. Harrington, D. R. Large, G. Burnett, and O. Georgiou, "Exploring the use of mid-air ultrasonic feedback to enhance automotive user interfaces," in *Proceedings of the 10th International Conference on Automotive User Interfaces and Interactive Vehicular Applications*, 2018, pp. 11–20.
- [12] H. Limerick, R. Hayden, D. Beattie, O. Georgiou, and J. Müller, "User engagement for mid-air haptic interactions with digital signage," in *Proceedings of the 8th ACM International Symposium on Pervasive Displays*, 2019, pp. 1–7.
- [13] R. Hirayama, D. M. Plasencia, N. Masuda, and S. Subramanian, "A volumetric display for visual, tactile and audio presentation using acoustic trapping," *Nature*, vol. 575, no. 7782, pp. 320–323, 2019.
- [14] R. Morales, I. Ezcuardia, J. Irisarri, M. A. B. Andrade, and A. Marzo, "Generating airborne ultrasonic amplitude patterns using an open hardware phased array," *Applied Sciences*, vol. 11, no. 7, 2021. [Online]. Available: <https://www.mdpi.com/2076-3417/11/7/2981>
- [15] K. Hasegawa and H. Shinoda, "Aerial vibrotactile display based on multi-unit ultrasound phased array," *IEEE transactions on haptics*, vol. 11, no. 3, pp. 367–377, 2018.
- [16] G. Torr, "The acoustic radiation force," *American Journal of Physics*, vol. 52, no. 5, pp. 402–408, 1984.
- [17] T. Iwamoto, M. Tatezono, and H. Shinoda, "Non-contact method for producing tactile sensation using airborne ultrasound," in *Proceedings of the 6th International Conference on Haptics: Perception, Devices and Scenarios*, ser. EuroHaptics '08. Berlin, Heidelberg: Springer-Verlag, 2008, p. 504–513. [Online]. Available: [https://doi.org/10.1007/978-3-540-69057-3\\_64](https://doi.org/10.1007/978-3-540-69057-3_64)
- [18] R. Morales González, A. Marzo, E. Freeman, W. Frier, and O. Georgiou, "Ultrapower: Powering tangible & wearable devices with focused ultrasound," in *Proceedings of the Fifteenth International Conference on Tangible, Embedded, and Embodied Interaction*, ser. TEI '21. New York, NY, USA: Association for Computing Machinery, 2021. [Online]. Available: <https://doi.org/10.1145/3430524.3440620>
- [19] I. Hwang, H. Son, and J. R. Kim, "Airpiano: Enhancing music playing experience in virtual reality with mid-air haptic feedback," in *2017 IEEE World Haptics Conference*. IEEE, 2017, pp. 213–218.
- [20] Y. Monnai, K. Hasegawa, M. Fujiwara, K. Yoshino, S. Inoue, and H. Shinoda, "Haptomime: Mid-air haptic interaction with a floating virtual screen," in *Proceedings of the 27th Annual ACM Symposium on User Interface Software and Technology*, ser. UIST '14. New York, NY, USA: Association for Computing Machinery, 2014, p. 663–667. [Online]. Available: <https://doi.org/10.1145/2642918.2647407>
- [21] S. Frish, M. Maksymenko, W. Frier, L. Corenthy, and O. Georgiou, "Mid-air haptic bio-holograms in mixed reality," in *2019 IEEE International Symposium on Mixed and Augmented Reality Adjunct (ISMAR-Adjunct)*. IEEE, 2019, pp. 348–352.
- [22] R. Morales, A. Marzo, S. Subramanian, and D. Martínez, "Leviprops: Animating levitated optimized fabric structures using holographic acoustic tweezers," in *Proceedings of the 32nd Annual ACM Symposium on User Interface Software and Technology*, ser. UIST '19. New York, NY, USA: Association for Computing Machinery, 2019, p. 651–661. [Online]. Available: <https://doi.org/10.1145/3332165.3347882>
- [23] S. Suzuki, R. Takahashi, M. Nakajima, K. Hasegawa, Y. Makino, and H. Shinoda, "Midair haptic display to human upper body," in *2018 57th Annual Conference of the Society of Instrument and Control Engineers of Japan (SICE)*. IEEE, 2018, pp. 848–853.

- [24] T. Howard, M. Marchal, A. Lécuyer, and C. Pacchierotti, "Pumah: Pantilt ultrasound mid-air haptics for larger interaction workspace in virtual reality," *IEEE Transactions on Haptics*, vol. 13, no. 1, pp. 38–44, 2020.
- [25] A. Sand, I. Rakkolainen, P. Isokoski, J. Kangas, R. Raisamo, and K. Palovuori, "Head-mounted display with mid-air tactile feedback," in *Proceedings of the 21st ACM Symposium on Virtual Reality Software and Technology*, 2015, pp. 51–58.
- [26] A. Price and B. Long, "Fibonacci spiral arranged ultrasound phased array for mid-air haptics," in *2018 IEEE International Ultrasonics Symposium (IUS)*, 2018, pp. 1–4.
- [27] A. Nashel and S. Razzaque, "Tactile virtual buttons for mobile devices," in *CHI '03 Extended Abstracts on Human Factors in Computing Systems*, ser. CHI EA '03. New York, NY, USA: Association for Computing Machinery, 2003, p. 854–855. [Online]. Available: <https://doi.org/10.1145/765891.766032>
- [28] J. R. Kim, X. Dai, X. Cao, C. Picciotto, D. Tan, and H. Tan, "A masking study of key-click feedback signals on a virtual keyboard," vol. 7282, 06 2012.
- [29] S. Rümelin, T. Gabler, and J. Bellenbaum, "Clicks are in the air: How to support the interaction with floating objects through ultrasonic feedback," *Proceedings of the 9th International Conference on Automotive User Interfaces and Interactive Vehicular Applications*, 2017.
- [30] M. Marchal, G. Gallagher, A. Lécuyer, and C. Pacchierotti, "Can stiffness sensations be rendered in virtual reality using mid-air ultrasound haptic technologies?" in *EUROHAPTICS 2020*, 2020.
- [31] M. Ito, Y. Kokumai, and H. Shinoda, "Midair click of dual-layer haptic button," in *2019 IEEE World Haptics Conference*. IEEE, 2019, pp. 349–352.
- [32] C. Ozkul, D. Geerts, and I. Rutten, "Combining auditory and mid-air haptic feedback for a light switch button," in *Proceedings of the 2020 International Conference on Multimodal Interaction*, ser. ICMI '20. New York, NY, USA: Association for Computing Machinery, 2020, p. 60–69. [Online]. Available: <https://doi.org/10.1145/3382507.3418823>
- [33] E. Freeman, D. Vo, and A. Brewster, "Haptiglow: Helping users position their hands for better mid-air gestures and ultrasound haptic feedback," in *2019 IEEE World Haptics Conference*, 2019, pp. 289–294.
- [34] A. Marzo, T. Corkett, and B. W. Drinkwater, "Ultrair: An open phased-array system for narrowband airborne ultrasound transmission," *IEEE transactions on ultrasonics, ferroelectrics, and frequency control*, vol. 65, no. 1, pp. 102–111, 2017.
- [35] H. T. O'Neil, "Theory of focusing radiators," *The Journal of the Acoustical Society of America*, vol. 21, no. 5, pp. 516–526, 1949. [Online]. Available: <https://doi.org/10.1121/1.1906542>
- [36] S. Mizutani, S. Suzuki, A. Matsubayashi, T. Morisaki, Y. Toide, Y. M. Masahiro Fujiwara, and H. Shinoda, "Use of multiple frequencies of ultrasound in midair haptic stimulation," in *Proceedings of the 9th International Conference on Automotive User Interfaces and Interactive Vehicular Applications*. Springer, 2022, pp. 66–74.
- [37] J. Chilles, W. Frier, A. Abdouni, M. Giordano, and O. Georgiou, "Laser doppler vibrometry and fme simulations of ultrasonic mid-air haptics," in *2019 IEEE World Haptics Conference*. IEEE, 2019, pp. 259–264.
- [38] S. Rümelin, T. Gabler, and J. Bellenbaum, "Clicks are in the air: how to support the interaction with floating objects through ultrasonic feedback," in *Proceedings of the 9th International Conference on Automotive User Interfaces and Interactive Vehicular Applications*, 2017, pp. 103–108.
- [39] D. Ablart, W. Frier, H. Limerick, O. Georgiou, and M. Obrist, "Using ultrasonic mid-air haptic patterns in multi-modal user experiences," in *2019 IEEE International Symposium on Haptic, Audio and Visual Environments and Games (HAVE)*. IEEE, 2019, pp. 1–6.
- [40] P. J. Westervelt, "Parametric acoustic array," *The Journal of the Acoustical Society of America*, vol. 35, no. 4, pp. 535–537, 1963.
- [41] H. Berkta and D. Leahy, "Farfield performance of parametric transmitters," *The Journal of the Acoustical Society of America*, vol. 55, no. 3, pp. 539–546, 1974.
- [42] F. J. Pompei, "The use of airborne ultrasonics for generating audible sound beams," *Journal of the Audio Engineering Society*, vol. 47, no. 9, pp. 726–731, 1999.
- [43] S. Suzuki, M. Fujiwara, Y. Makino, and H. Shinoda, "Reducing amplitude fluctuation by gradual phase shift in midair ultrasound haptics," *IEEE Transactions on Haptics*, vol. 13, no. 1, pp. 87–93, 2020.
- [44] S. Carcagno, A. Di Battista, and C. J. Plack, "Effects of high-intensity airborne ultrasound exposure on behavioural and electrophysiological measures of auditory function," *Acta Acustica united with Acustica*, vol. 105, no. 6, pp. 1183–1197, 2019.
- [45] A. Di Battista, "The effect of 40 khz ultrasonic noise exposure on human hearing," in *Proc. 23rd Int. Cong. Acoustics*, 2019, pp. 4783–4788.
- [46] A. Raza, W. Hassan, T. Ogay, I. Hwang, and S. Jeon, "Perceptually correct haptic rendering in mid-air using ultrasound phased array," *IEEE Transactions on Industrial Electronics*, vol. 67, no. 1, pp. 736–745, 2020.
- [47] L. Fan, A. Song, and H. Zhang, "Haptic interface device using cable tension based on ultrasonic phased array," *IEEE Access*, vol. 8, pp. 162 880–162 891, 2020.
- [48] C. E. Kandel, A. E. Simor, and D. A. Redelmeier, "Elevator buttons as unrecognized sources of bacterial colonization in hospitals," *Open Medicine*, vol. 8, no. 3, p. e81, 2014.
- [49] J. Pearson, G. Bailey, S. Robinson, M. Jones, T. Owen, C. Zhang, T. Reitmaier, C. Steer, A. Carter, D. R. Sahoo *et al.*, "Can't touch this: Rethinking public technology in a covid-19 era," in *CHI Conference on Human Factors in Computing Systems*, 2022, pp. 1–14.
- [50] T. Singhal and M. Phutane, "Elevating haptics: An accessible and contactless elevator concept with tactile mid-air controls," in *Extended Abstracts of the 2021 CHI Conference on Human Factors in Computing Systems*, 2021, pp. 1–4.
- [51] A. Kumar, D. C. Wong, H. C. Shen, and A. K. Jain, "Personal authentication using hand images," *Pattern Recognition Letters*, vol. 27, no. 13, pp. 1478–1486, 2006.

**Rafael Morales** received his BSc and MSc in Computer Science from the University of Malaga (Spain). He also has a PhD in Human-Computer Interaction from the University of Paris-Saclay (France). In 2017 he was a postdoc at the University of Sussex in the UK, working in acoustic levitation and emerging technologies. He then moved to industry working at Ultraleap Ltd as a Haptic research engineer for Levitate project. Rafael has been a key investigator in several European projects which lead to various publications in top-tier conferences (HCI, Digital Fabrication and Haptics). His main research is focused on emerging technologies in novel interactive systems.

**Dario Pittera** received his B.S. in Communication and Psychology (2011) and his M.S. in Clinical psychology, developmental psychology and neuropsychology (2014), both from the Università degli Studi di Milano-Bicocca, Milan, Italy. He worked as a researcher at the Policlinico di Milano Hospital (2013/2014) and at the University of Birmingham (2015/2016), investigating haptic technology through psychophysical experiments. He then worked as a Lab Associate at Disney Research, Pittsburgh, PA, US as a part of his PhD degree, received in 2019 at the University of Sussex working on mid-air haptics illusions and embodiment. Currently, he is working as a behavioural research scientist at Ultraleap. His research is focused on the perception and exploration of mid-air haptic technology.

**Orestis Georgiou** (Senior Member, IEEE) received a Ph.D. in Mathematics from the University of Bristol in 2012. In 2013 he was a postdoc at the Max Plack Institute of Complex Physics in Dresden. He then moved to the industry, first working for Toshiba Telecommunications Research Lab as a Senior Researcher (2013-2017), and later for Ultraleap as Head of R&D Partnerships (2017-present) where he is the PI on several publicly funded R&D projects. He is the author of 5 patents and over 80 academic papers published in leading journals and conferences of Mathematics, Physics, Computer Science, Engineering and Medicine. Orestis was awarded a Marie Curie Individual Fellowship hosted at the University of Cyprus (2019-2021), is an author of two best paper awards (ISWCS'2013 and AutoUI'2018) and is the recipient of the prestigious IEEE Heinrich Hertz Award in 2019.

**Brian Kappus** received his PhD in Physics from The University of California, Los Angeles (UCLA). Focusing on nonlinear acoustics, he studied the conversion of sound to light in university (sonoluminescence) followed in industry by designing devices to turn ultrasound to audible sound (directional audio) and finally ultrasound to force (haptics). Well versed in both theoretical and practical approaches to array acoustics, he currently leads the hardware and measurement groups at Ultraleap. He is the author of 11 academic publications in a variety of physics and medical journals and 30 issued or pending patents in the fields of signal processing, audio, ultrasound, and haptics.

**William Frier** received his PhD in Human-Computer Interaction from the University of Sussex and is now the Lead Haptics Researcher at Ultraleap. Since Ultraleap Ltd early days, he has been a key investigator in studying the perception of mid-air haptics which lead to various patents, and publications in HCI and Haptic conferences. He has studied Electrical and Electronics engineering at ESIGELEC (France) and Intelligent System and Robotics at University Pierre and Marie Curie (France), making him a key person in the development and integration of modular ultrasound mid-air haptic devices for robotic applications and Human-Machine Interfaces. William is the recipient of a UKRI Future Leader Fellowship and an honorary researcher at the University of Bristol.